doi.org/10.36721/PJPS.2026.39.6.161.1

Pharmacokinetic and biotransformation analysis of thiophene- and dichlorophenyl-substituted indole-3-butyric acid hydrazones

Sehar Madni[1,2], Aisha Rafique[1,3], Muhammad Usama Munir[1], Mahpara Gondal[1,4], Kanwal Rehman[5] and Muhammad Sajid Hamid Akash[1]*

[1]Department of Pharmaceutical Chemistry, Government College University, Faisalabad, Pakistan
[2]Alliant College of Professional Studies, Lahore, Pakistan
[3]Lords College of Pharmacy, Lahore, Pakistan
[4]Yashfeen College of Pharmacy, Yashfeen Education System, Lahore, Pakistan
[5]Department of Pharmacy, The Women University, Multan, Pakistan

Abstract: **Background**: The indole-3-butyric acid based hydrazones have gained attention due to their reported biological effectiveness; however, their *in-vivo* pharmacokinetic properties and metabolic pathways are yet inadequately investigated. Comprehending structure-dependent variations in absorption and metabolism is essential for the preliminary optimization of this scaffold. **Objectives**: The aim of the study was to comparatively assess the pharmacokinetics and biotransformation of two IBA-based hydrazones—4-indole-3-butane-(thiophen-2-ylmethylene) hydrazone (TIBH) and 1-(4-amino-3,5-dichlorophenyl) ethylidene-4-indole-3-butane hydrazone (DIBH) and to clarify the impact of structural substitution on their metabolic pathways *in-vivo*. **Methods**: UV–VIS spectrophotometry under verified linear circumstances assessed serum concentrations over 24 hr in healthy rats after a single oral dosage (10 mg/kg). Metabolites and temporal profiles were identified using LC–ESI–MS/MS. Biotransformer 3.0 was used for cheminformatic prediction of metabolic pathways and enzyme participation. In exploratory analysis, data are presented descriptively (mean ± SD). **Results**: TIBH demonstrated accelerated absorption with an earlier peak concentration (C_{max} at 4 hr) and a reduced half-life, while DIBH exhibited a delayed peak exposure (C_{max} at 8 hr) and extended systemic persistence. The LC–MS/MS study showed that both compounds went through a lot of Phase-I (hydrolysis, hydroxylation and deamination) and Phase-II (glucuronidation, sulfonation and acetylation) metabolism. This made them more polar and facilitating elimination. Different metabolite profiles showed how substitution changed metabolism. TIBH had faster oxidative and conjugative turnover, while DIBH was more stable with late stage dechlorination. The predicted routes and enzyme involvement aligned well with the experimental results. **Conclusion**: This research indicated that aromatic substitution significantly affects the pharmacokinetic and metabolic properties of IBA-based hydrazones. Despite its constraints due to an exploratory design and absence of pharmacological validation, the combined experimental and computational methodology offers mechanistic understanding of structure–metabolism connections and guides subsequent optimization and biological assessment of hydrazone scaffolds.

Keywords: Biotransformation; LC–MS/MS metabolomics; Metabolite profiling.

Submitted on 01-11-2025 – Revised on 17-01-2026 – Accepted on 21-01-2026

INTRODUCTION

Biotransformation and pharmacokinetics are important parts of drug development because they explain how drugs are broken down in the body and how these processes affect treatment (Lai *et al*., 2022). These are especially important for compounds that include hydrazones since their susceptibility to oxidative modification and hydrolytic cleavage is highly dependent on the electronic characteristics and structure of their substituents (Rafique *et al*., 2025).

Indole-3-butyric acid (IBA), an auxin, is a useful scaffold in pharmaceutical chemistry. The indole core makes it flat and allows hydrogen bonding and the butyric chain makes it more flexible and lipophilic. Available *in-vivo* pharmacokinetic studies on indole-based and hydrazone-containing compounds suggest that aromatic substitution plays a critical role in determining metabolic turnover, half-life and systemic exposure. However, most reports focus on single compound and direct comparative pharmacokinetic evaluations of closely related analogs with distinct aromatic features remain scarce (Babalola *et al*., 2025; Munir *et al.*, 2025) yet *in-vivo* metabolism and pharmacokinetics remain underreported, critical for predicting bioavailability and safety. Despite the reported biological activities of indole-based hydrazones, it remains unclear how specific aromatic substitutions influence their *in-vivo* pharmacokinetic behavior and metabolic fate. In particular, systematic comparative data linking heteroaromatic and halogenated substituents to absorption, clearance and biotransformation pathways are limited. The present study was therefore designed to test the hypothesis that thiophene and dichlorophenyl substitutions differentially affect oral exposure, metabolic stability and clearance of IBA hydrazones *in-vivo*.

**Corresponding author:* e-mail: sajidakash@gcuf.edu.pk

Four IBA-hydrazones were produced through the condensation of IBA hydrazide with aldehydes or ketones under reflux conditions. Structural investigation using UV, FTIR, NMR and MS confirmed their purity and integrity. Biological screening showed enzyme inhibition and anticancer potential consistent with docking. Among the synthesized analogs, TIBH (thiophene containing moiety) and DIBH (amino dichloro phenyl containing moiety) were selected to explore substituent-dependent pharmacokinetic behavior. The thiophene ring in TIBH represents a heteroaromatic moiety commonly associated with oxidative metabolism, whereas the dichlorophenyl group in DIBH was chosen to examine the influence of halogenation on metabolic stability and systemic persistence (Madni *et al*., 2025; Rafique *et al*., 2025). Early pharmacokinetic screening uses UV–VIS spectrophotometry for C_{max}, T_{max}, AUC and $t_{1/2}$ estimation (Karnakar *et al*. 2020; Akash *et al*., 2020) while LC–MS/MS is required for trace-level metabolite structural elucidation. Computational tools complement experiments; Biotransformer 3.0 predicts CYP and microbiota-mediated transformations (Djoumbou-Feunang *et al*., 2019). On this basis, the present work aimed to comparatively evaluate the *in-vivo* pharmacokinetics and biotransformation of TIBH and DIBH using UV–VIS-based exposure estimation, LC–MS/MS metabolite profiling and *in-silico* metabolic prediction, with the objective of elucidating structure-dependent differences in metabolic disposition.

MATERIALS AND METHODS

Chemicals and reagents

All reagents and solvents used in the study were of analytical grade and employed without additional purification.

Acute safety profile assessment

Acute oral toxicity was evaluated in Swiss albino rats following OECD Guideline 425. Animals were fasted overnight and administered a single oral dose of the test compound by gavage in a stepwise manner (n = 3 per dose level). Animals were observed continuously for the first 4 hrs and then daily for 14 days for clinical signs of toxicity. Body weights were recorded on days 0, 7 and 14 and mortality and adverse effects were monitored to determine the acute toxicity profile (Guideline 425., 2001).

Preparation of IBA hydrazones solution

IBA-derived hydrazones DIBH and TIBH were dissolved in sterile normal saline at 10 mg/kg and homogenized through weighing, dissolving and sonicating. A non-toxic, analytically detectable oral dose of 10 mg/kg was chosen for exploratory pharmacokinetic and metabolite profiling, based on procedure parameters and safety testing. The rats were given 1 mL doses via oral gavage, calibrated to their body weight for precise dosing (Madni *et al*., 2025).

Experimental design

A 24 h pharmacokinetic and metabolite profiling investigation was conducted in Swiss albino rats. There were three independent animals (n = 3) in each experimental group. Rats were housed at 22 ± 2 °C, 55 ± 5% RH, 12 hr light/dark with free access to chow and water. After overnight fast, rats received DIBH or TIBH (10 mg/kg) orally. Blood (1 mL) was collected via cardiac puncture into EDTA tubes at 4, 8, 12 and 24 hr. Sampling at 4, 8, 12 and 24 hr was performed in accordance with the predefined exploratory pharmacokinetic protocol to assess comparative exposure and metabolic progression. Samples were centrifuged at 4,500 × g for 5 min; serum stored at −20 °C. Performed in biological triplicate, samples analyzed separately for drug concentration and metabolites. Mean ± SD was calculated to present pharmacokinetic and metabolomic data (Rafique *et al*., 2025; Gondal *et al.*, 2025).

Determination of pharmacokinetic parameters

Serum concentrations of orally administered IBA hydrazone derivatives (DIBH and TIBH) were quantified by UV–VIS spectrophotometry using a calibration curve from standards of 20–100 µg/mL. Absorbance versus concentration gave linear regression (A = mC + b); unknown concentrations were calculated as C = (A − b)/m at 4, 8, 12 and 24 h post-dose (Tariq *et al*., 2015). Pharmacokinetic parameters were derived via a one-compartment model with first-order elimination: elimination constant k from the terminal slope, $t_{1/2}$ = 0.693/k and $AUC_{\sigma\text{-}24}$ by the trapezoidal rule. C_{max} and T_{max} were observed; CL = Dose/$AUC_{\sigma\text{-}24}$ and Vd = CL/k were estimated, respectively, in rats (Ahn *et al*., 2011).

LC-MS/MS-based metabolite profiling

Metabolomic profiling of serum samples used LC–MS/MS to identify biotransformation products of IBA-derived hydrazones. 10 µL serum were mixed with four volumes ice-cold acetonitrile, vortexed and centrifuged at 16,000×g for 15 min. The supernatant was evaporated under nitrogen, reconstituted in 20 µL methanol, centrifuged and 10 µL injected for LC–MS/MS analysis. Profiling used an Agilent 6495C Triple Quadrupole with electrospray ionization coupled to a Zorbax Extend-C18 column (2.1×100 mm, 1.8 µm). Mobile phases were 0.1% formic acid in water (A) and acetonitrile (B) with a gradient from 2% to 98% B over 16 min; Flow 0.35 mL/min; column 40 °C. The mass spectrometer operated in positive-ion mode across m/z 20–500. Source conditions included capillary voltage 3,000 V, nozzle voltage 1,500 V, sheath gas 300 °C, 6 L/min and auxiliary gas 14 L/min (Gondal *et al*., 2025). Full-scan spectra (m/z 50–500) were acquired at 3.0 kV and selected precursor ions were fragmented by collision-induced dissociation (20–30 eV) for structural elucidation, confirmation and robust reproducibility.

In-silico metabolite prediction

In-silico metabolic prediction was performed by using Biotransformer version 3.0 in Human Super Transform mode (https://Biotransformer.ca), a cheminformatics tool integrating machine-learning and rule-based models to simulate human/microbial metabolism (Wishart *et al*., 2022). DIBH and TIBH canonical SMILES were submitted as input to predict Phase-I (oxidation, reduction, hydrolysis) and Phase-II (sulfation, glucuronidation, methylation) and microbiota-mediated metabolites prioritized for experimental validation. Predicted metabolites were validated by matching theoretical m/z values and proposed biotransformation with experimentally observed LC–MS/MS parent ions and fragmentation patterns.

Statistical analysis

Pharmacokinetic parameters were calculated and graphically evaluated using Microsoft Excel 365. Concentration–time data are expressed as mean ± standard deviation (SD) to summarize T_{max}, C_{max} and $AUC_{\sigma\text{-}24}$ values for TIBH and DIBH. Log-transformed plasma concentration data were analyzed by linear regression to assess first-order elimination kinetics and to confirm consistency with a one-compartment pharmacokinetic model.

RESULTS

Acute oral toxicity assessment

Acute oral toxicity in Swiss albino rats receiving single doses of DIBH or TIBH up to 2000 mg/kg revealed no mortality or overt distress over 14 days; animals maintained normal behavior, food intake and steady weight gain, indicating low toxicity.

Analysis of pharmacokinetic parameters

Pharmacokinetic evaluation of DIBH and TIBH over 24 hrs following a single 10 mg/kg oral dose revealed distinct absorption and elimination profiles as given in table 1. Serum concentrations were estimated by UV–VIS spectrophotometry using calibration exhibiting good linearity $R^2 > 0.99$. For DIBH, the calibration curve showed a slope of 0.0022 ± 0.001 absorbance units per µg/mL with an intercept of 0.0617 ± 0.002, while TIBH exhibited a slope of 0.00194 ± 0.008 absorbance units per µg/mL and an intercept of 0.078 ± 0.003, confirming analytical consistency within the tested concentration range.

TIBH reached peak concentration earlier (C_{max} = 104.5 ± 5.0 µg/ml at 4 hr), whereas DIBH showed delayed peak exposure (C_{max} = 101.0 ± 4.5 µg/ml at 8 h), indicating slower absorption. Elimination rate constants were 0.098 ± 0.007 h^{-1} for TIBH and 0.060 ± 0.005 h^{-1} for DIBH, corresponding to half-lives of 7.06 ± 0.51 h and 11.5 ± 0.95 h, respectively. The $AUC_{\sigma\text{-}24}$ values for TIBH and DIBH were 883 ± 0.45 µg·h/mL and 854 ± 0.32 µg·h/ml, respectively. This means that both drugs had similar overall exposure, but DIBH stayed in the body longer. The longer mean residence time for DIBH (16.7 ± 1.3 h) compared to TIBH (11.3 ± 0.8 h) supports the idea that systemic clearance is slower.

LC-MS/MS-based metabolite profiling

Metabolite profiling of DIBH

LC-MS/MS study of serum after oral DIBH treatment showed a time-dependent metabolic process, including Phase-I oxidation and Phase-II conjugation. In the early stages of metabolism (4 hr), hydrolytic breakdown of the hydrazone linkage and oxidative transformations produced low-molecular-weight indole fragments (m/z 104.1 and 149.0) and oxidized intermediates (Fig. 1). Early metabolites occurred briefly and reduced later, indicating fast clearance of polar breakdown products (Table 2). N-demethylated and hydroxylated derivatives (m/z 358.3 and 429.3) indicate that oxidative metabolism increased throughout the intermediate period (8–12 hr). These metabolites are CYP-mediated Phase-I biotransformations that improve polarity and prepare molecules for conjugation. The parent molecule (m/z 402.3) was detected 12 hr post-dose (Fig. 1), demonstrating good absorption and metabolic stability before conversion into oxidized intermediates. Advanced detoxification was indicated by the predominance of highly polar terminal metabolites at later stages (24 hr). These included a glucuronide conjugate (m/z 556), formed via UDP-glucuronosyltransferase-mediated Phase-II conjugation following prior oxidation, as well as a dechlorinated oxidative derivative (m/z 370.2) arising from combined deamination and dechlorination. The presence of a neutral dihydroxylated metabolite (m/z 421.2) indicates late-stage oxidative metabolism and increased renal elimination readiness. At intermediate time intervals, a polyhydroxylated oxidized product (m/z 455.3) indicated significant oxidative processing before terminal clearance (Fig. 1). The compound's systematic biotransformation pathway—hydrazone cleavage, progressive oxidative modification and conjugation-mediated detoxification extends systemic retention and pharmacokinetic elimination.

Metabolite profiling of TIBH

LC–MS/MS analysis of serum following oral administration of TIBH revealed rapid and extensive biotransformation involving sequential Phase-I oxidation and Phase-II conjugation as given in table 2. At early time points (4–8 hr), metabolism was dominated by hydrazone cleavage and indole ring fragmentation, producing low-molecular-weight indole-derived species (m/z 105.0 and 149.0) and thiophene-containing fragments (m/z 226.1). These metabolites appeared transiently and declined by 12 hr, indicating rapid degradation and clearance of polar cleavage products (Fig. 2). During the intermediate phase (8–12 hr), oxidative metabolism became more prominent, as evidenced by hydroxylated and partially cleaved intermediates (m/z 237.1, 327.2 and 297.1).

Table 1: Evaluation of pharmacokinetic parameters of DIBH and TIBH

Pharmacokinetic parameters	DIBH (Mean ± SD)	TIBH (Mean ± SD)
Slope (absorbance/concentration)	0.0022 ± 0.001	0.00194 ± 0.008
Intercept	0.0617 ± 0.002	0.078 ± 0.003
Maximum concentration C_{max} (µg/ml)	101.0 ± 4.5	104.5 ± 5.0
Time to peak concentration T_{max} (h)	8 ± 0.02 h	4 ± 0.01 h
Elimination rate constant K_{ele} (h^{-1})	0.060 ± 0.005	0.098 ± 0.007
Plasma half-life ($t_{1/2}$, h)	11.5 ± 0.95	7.06 ± 0.51
Area under curve AUC 0-24h (µg h/ml)	854 ± 0.32	883 ± 0.45
Clearance CL (ml/h)	11.7 ± 0.64	11.3 ± 0.58
Volume of distribution Vd (ml)	19.5 ± 0.012	11.5 ± 0.010
Mean residence time MRT (h)	16.7 ± 1.3	11.3 ± 0.8

Table 2: Comparative analysis of all metabolites identified by LCMS/MS after DIBH and TIBH biotransformation.

Compound	m/z	Identified metabolites	Peak intensity	Proposed biotransformation
DIBH	104.1	3-Aminoindole fragment	Increased at 4 hr, decreased by 8 hr	Cleavage at hydrazone bond
	149	Hydrolyzed indole fragment	Increased at 4 hr, decreased by 12 hr	Cleavage of aryl-indole bond
	358.3	N-Demethylated metabolite	Increased from 4 hr to 8 hr, decreased by 12 hr	N-demethylation and oxidation
	402.3	Parent DIBH	Detected 4-12 hr, decreased over time	Unmodified parent molecule
	429.3	Protonated Di hydroxylated DIBH	Increased at 4 hr, persisted to 12 hr	Phase-I Hydroxylation
	455.3	Polyhydroxylated derivative	Moderate from 4-12 hr	Multiple hydroxylation and oxidation
	556.3	Glucuronide conjugate	Increased at 8 hr; persists to 24 hr	Phase-II Glucuronidation
	370.2	Deaminated-Dechlorinated product	Only at 24 hr	Deamination and dechlorination of aryl ring
	421.2	Neutral dihydroxylated fragment	Detected at 24 hr	Dihydroxylated species
TIBH	313.2	Parent TIBH	Increased at 4 hr, decreased by 12 hr	Unmodified parent molecule
	105	Indole-Amine Fragment	Increased at 4 hr, decreased by 12 hr	Hydrazone cleavage forming amino-indole
	149	Indole fragment Ion	Increased at 4 hr, highly decreased by 24 hr	Indole cleavage fragment
	226.1	Thiophene-Hydrazone fragment	Only at 4 hr	Indole ring loss leaving thiophene-hydrazone
	237.1	Indole-Hydrazide fragment	Increased at 8 hr; persists to 12 hr	Cleavage and Phase-I hydroxylation
	327.2	Mono-Hydroxylated TIBH	Increased at 8 hr, decreased by 12 hr	Phase-I Hydroxylation
	297.1	Dihydroxylated cleaved metabolite	Peak at 12 hr	Oxidative fragmentation and dihydroxylation
	371.1	Acetylated hydroxy-TIBH	Increased at 8 hr, decreased by 12 hr	Phase-II Acetylation after hydroxylation
	457.3	Hydroxy-Sulfonyl-Acetylated metabolite	Increased at 8 hr, decreased by 12 hr	Phase-II Conjugation with Acetyl + sulfonyl groups
	496.2	Hydroxy-Glucuronide TIBH	Only at 24 hr	Phase-II Glucuronidation after hydroxylation

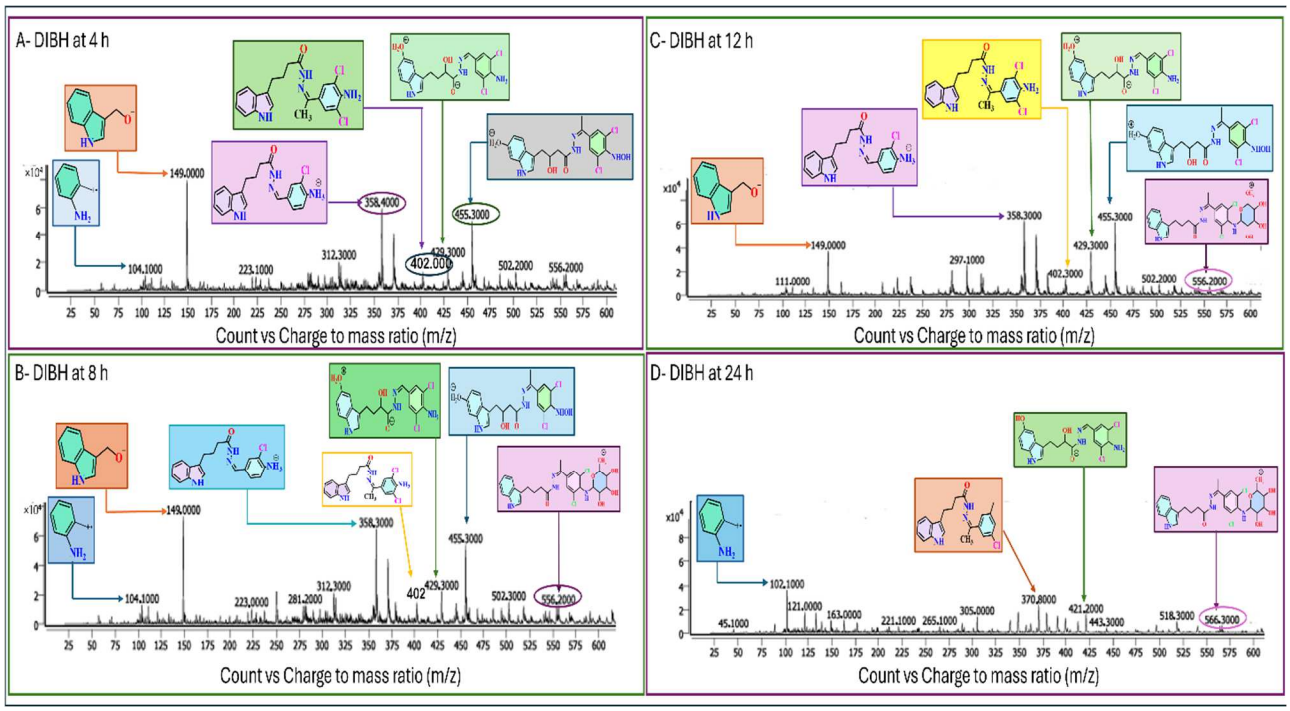

Fig. 1: LC-MS/MS spectra of DIBH at 4, 8, 12, 24 h post-administration. Progressive appearance of oxidized (m/z 358.4, 429.3, 455.3) and glucuronidated (m/z 556.2) metabolites indicates ongoing Phase-I and Phase II biotransformation.

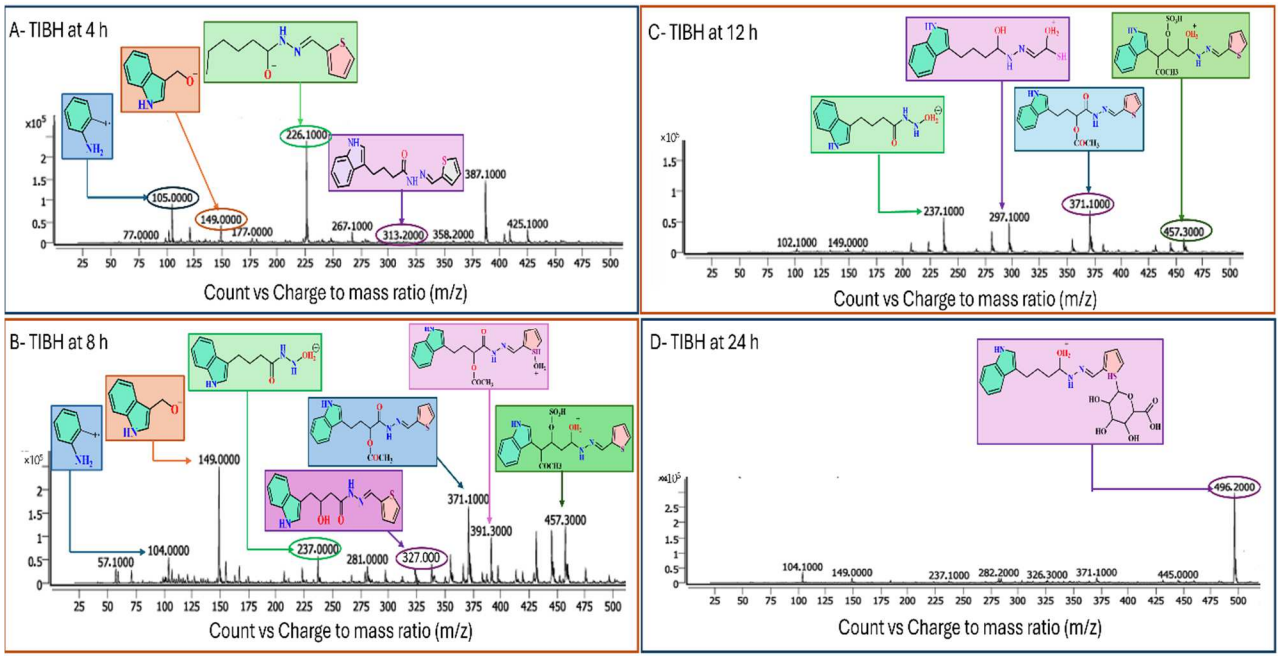

Fig. 2: LC-MS/MS spectra of TIBH at 4, 8, 12, 24 hr post-administration. At 4 hr, parent compound (m/z 313.2) and early cleavage fragments (m/z 105.0, 149.0, 226.1) dominate, while at 8 hr, oxidized (m/z 237.1, 327.2) and conjugated metabolites (m/z 371.1, 457.3) reflect progressive biotransformation.

This change involves CYP-mediated oxidation of the hydrazide linker and thiophene or alkyl sections, leading to increased polarity and easier conjugation. The parent molecule (m/z 313.2) was most abundant at 4 hr and gradually decreased, becoming undetectable by 24 hr (Fig. 2), indicating efficient absorption and quick metabolic conversion. Conjugated metabolites became more abundant later, indicating detoxification. Acetylated and sulfonated derivatives (m/z 371.1 and 457.3) were predominantly observed between 8 and 12 hr, when Phase-II metabolism peaks.

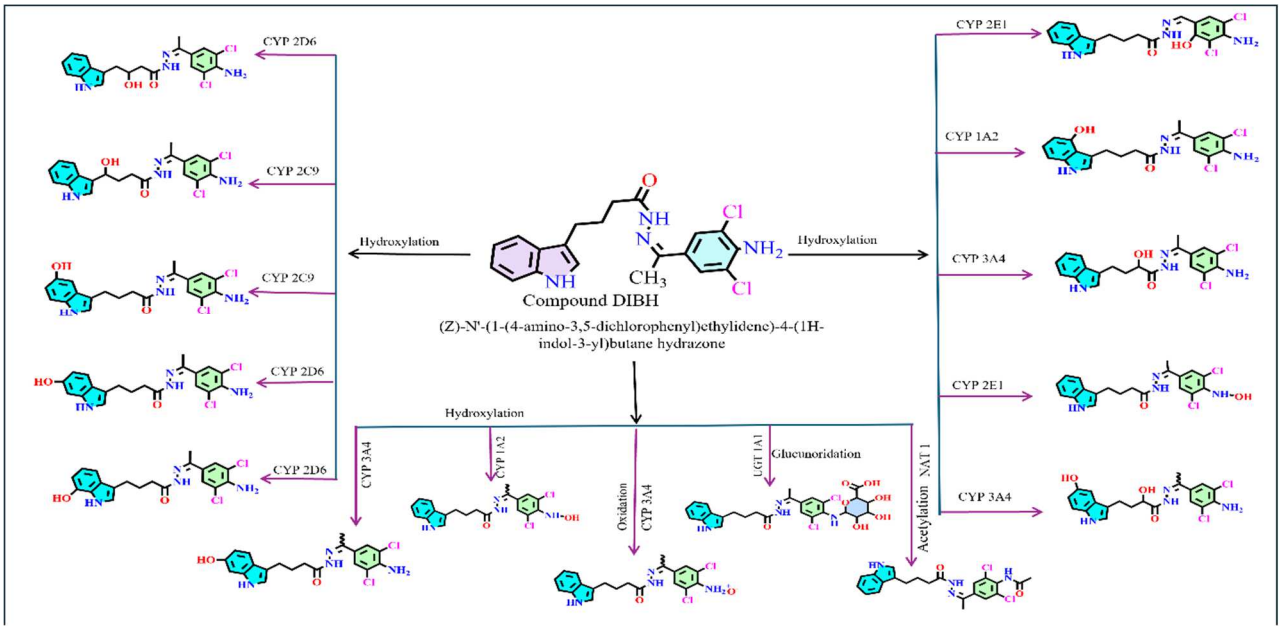

Fig. 3: Biotransformer 3.0 predicted DIBH metabolic pathways. CYP450-mediated hydroxylation, oxidation and conjugation reveal DIBH's suggested biotransformation profile.

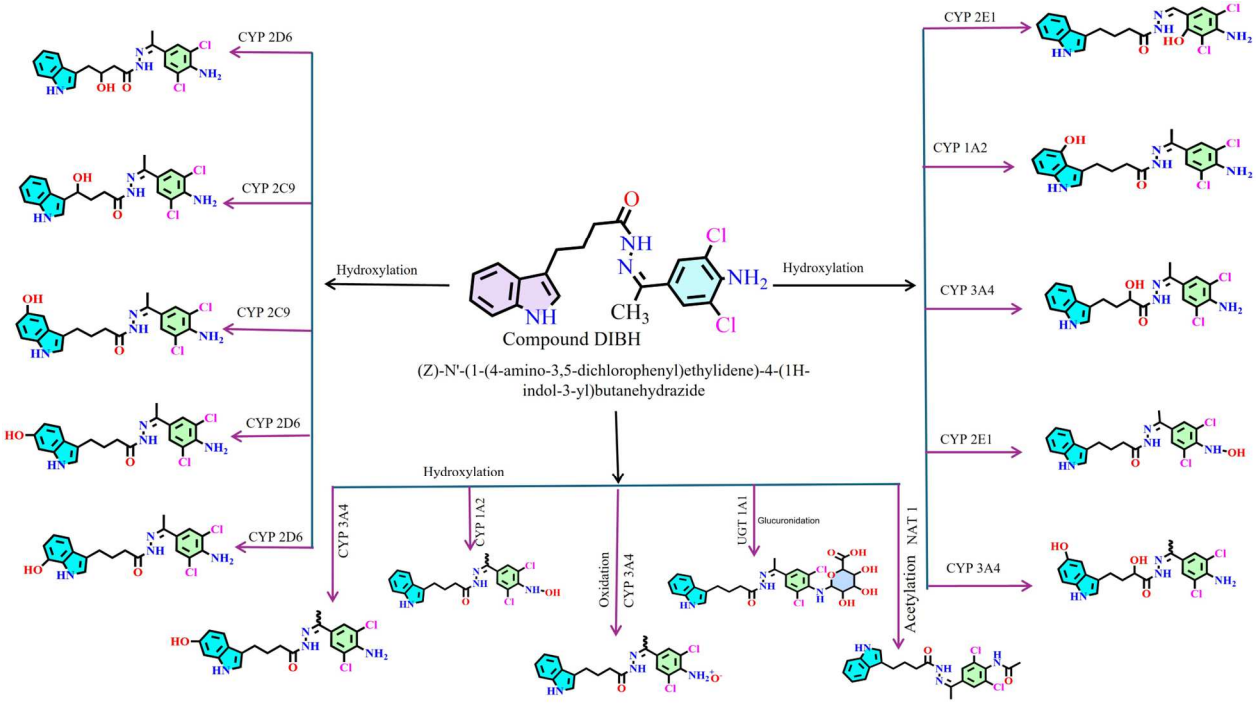

Fig. 4: Biotransformer 3.0 TIBH metabolic pathway predictions. The model forecasts CYP- and FMO-mediated hydroxylation, oxidation, and conjugation processes, yielding various metabolites for TIBH biotransformation.

A highly polar metabolite that favors renal or biliary clearance is produced when biotransformation completes with a hydroxy-glucuronide molecule (m/z 496) at 24 hr (Fig. 2). Since TIBH broke down quickly and altered through oxidation and conjugation, it had a quicker metabolic turnover and shorter systemic persistence than DIBH.

Prediction of drug metabolism

Predicted metabolic transformations of DIBH

Biotransformer 3.0 predicted multiple CYP450-mediated (CYP1A2, CYP2D6, CYP2E1, CYP2C9, CYP3A4) pathways for DIBH metabolism as shown in figure 3.

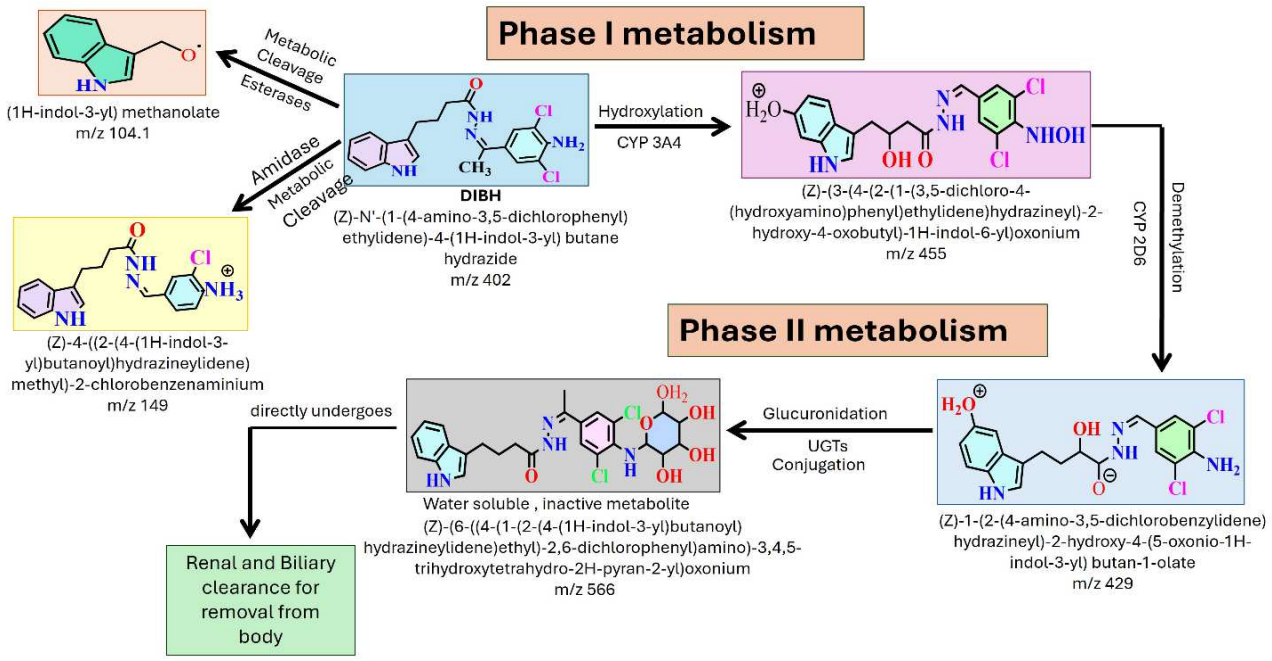

Fig. 5: Proposed metabolic pathway of DIBH.

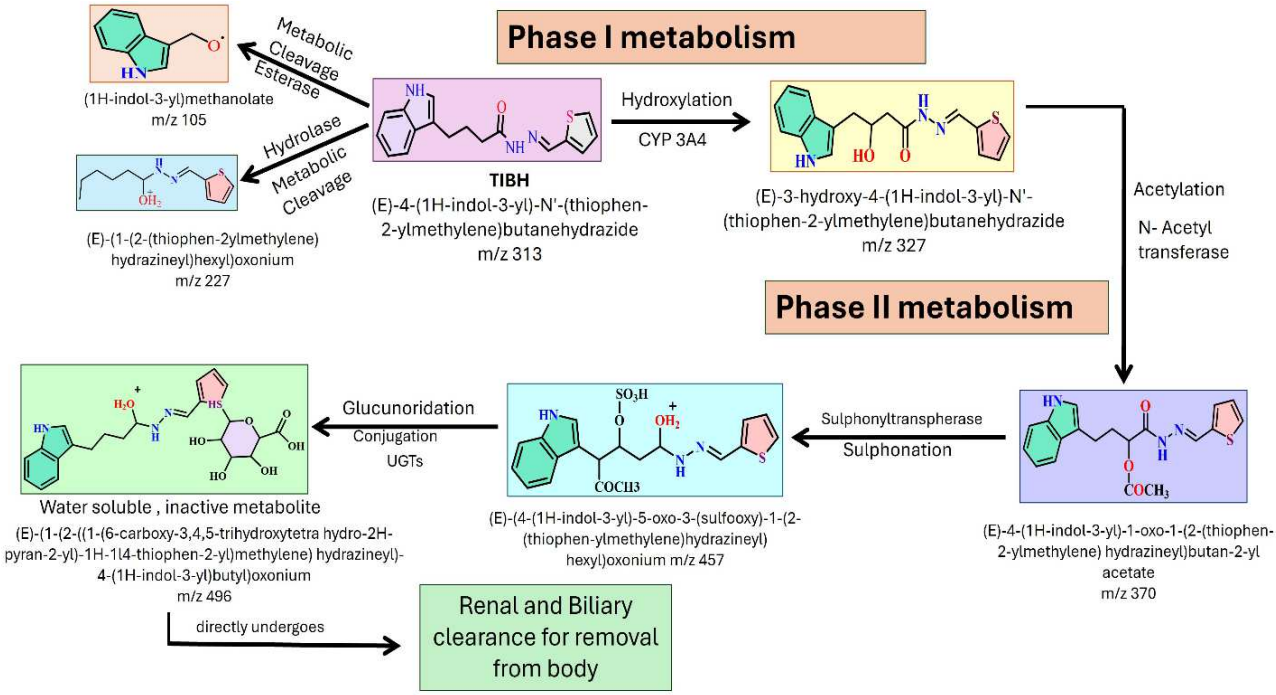

Fig. 6: Proposed metabolic pathway of TIBH.

The Phase-I hydroxylation of indole, dichlorophenyl and butyl regions improves solubility and excretion, while Phase-II conjugations—UGT1A1-mediated glucuronidation and NAT1-driven acetylation—DIBH undergoes intensive hepatic biotransformation (Fig. 3).

Predicted metabolic transformations of TIBH

Biotransformer 3.0 predicted extensive CYP1A2, CYP2D6, CYP2C9, CYP3A4 and FMO3-mediated metabolism of TIBH. In Phase-I, indole hydroxylation, thiophene oxidation and epoxidation produced sulfoxides and N-oxides. The active CYP/FMO3-driven hepatic

transformation of these intermediates caused conjugation (Fig. 4).

DISCUSSION

This research offered a comprehensive assessment of the *in-vivo* pharmacokinetics and metabolic characteristics of the IBA hydrazones (TIBH and DIBH) by pharmacokinetic profiling, LC–MS/MS analysis, cheminformatic prediction and suggested metabolic pathways. Prior studies have established the antioxidant and anticancer properties of IBA-based hydrazones; however, their *in-vivo* metabolic disposition has not been thoroughly investigated (Madni *et al*., 2025; Akash *et al*., 2023). This study fills the gap by connecting structural characteristics with pharmacokinetic behavior and biotransformation processes.

The different pharmacokinetic profiles of TIBH and DIBH can be explained by their proposed metabolic routes (Figs. 5 and 6). TIBH was quickly absorbed and was not retained for long in the body. This is in line with the metabolic route shown in figure 6, where early hydrazone cleavage and CYP-mediated oxidation are the main processes. The thiophene substituent makes the molecule more likely to go through oxidative metabolism, which speeds up the synthesis of polar intermediates that can easily go through Phase-II conjugation, such as acetylation, sulfonation and glucuronidation. These changes explain why parent TIBH levels drop quickly and conjugated metabolites take over later on, which supports its quicker clearance profile.

On the other hand, DIBH showed delayed absorption and longer systemic exposure, as seen by its longer half-life and higher apparent distribution volume. The amino dichlorophenyl part of DIBH makes it more stable in the body and less likely to be attacked by oxidative agents early on. This is a common effect seen in halogenated aromatic systems (Fig. 5). Hydroxylation and N-demethylation are the first steps in the Sequential Phase-I process, which comes before late-stage deamination and dechlorination. The identification of a deaminated–dechlorinated metabolite (m/z 370.2) at 24 hr signifies extensive oxidative processing, aligning with halogen removal as a last detoxification step. This delayed metabolic process offers a molecular foundation for the persistent systemic presence of DIBH (Rafique *et al*., 2025; Guengerich *et al*., 2018).

The robust correlation between Biotransformer 3.0 predictions and experimentally identified metabolites reinforces the suggested pathways illustrated in figures 5 and 6. The predicted roles of CYP3A4, CYP2D6, CYP2C9 and CYP1A2 match the oxidative and demethylation reactions that were seen. UGT1A1- and NAT1-mediated conjugation explains how glucuronide and acetylated metabolites are made. This agreement between the *in-silico* prediction and the LC–MS/MS data assures that the metabolic pathways for both substances are in the liver. This study was performed as an exploratory examination, with limitations including a restricted sample size, potential analytical sensitivity issues and ambiguity in the postulated metabolic pathways based on indirect evidence. In general, combining pharmacokinetic characteristics with metabolomic profiling and suggested biotransformation schemes shows how little variations in structure between TIBH and DIBH affect how they act in living organisms. TIBH's fast oxidative and conjugative metabolism makes it a good candidate for short-acting or acute therapeutic uses, whereas DIBH's slower clearance and longer exposure may make it better for long-term therapeutic techniques. These results show how important it is to undertake metabolic pathway study early on when trying to improve IBA hydrazones as therapeutic candidates.

CONCLUSION

This study offers a comparative evaluation of the *in-vivo* pharmacokinetics and metabolic disposition of the IBA hydrazones TIBH and DIBH by pharmacokinetic profiling, LC–MS/MS-based metabolite analysis and cheminformatic prediction. Different pharmacokinetic characteristics were seen. TIBH had a faster absorption and clearance, while DIBH had a slower uptake and longer systemic persistence, which matched their structural replacement patterns. Both compounds underwent substantial Phase-I and Phase-II metabolism, resulting in enhanced polarity and aiding renal and biliary clearance.

Combining experimental and *in-silico* data made it possible to suggest possible biotransformation pathways and show how aromatic substitution affects metabolic stability and clearance. However, the results are just for pharmacokinetic and metabolic characterization because no direct pharmacodynamic or effectiveness evaluation was done. This study was exploratory in nature and involved a limited sample size and metabolite identification relied on LC–MS/MS fragmentation patterns and computational prediction rather than isolated standards. Future studies should focus on quantitative evaluation of major metabolites, expanded pharmacokinetic analysis and targeted biological assays to further support optimization of indole-based hydrazones in early-stage drug development.

Acknowledgments
N/A

Authors' contributions
Sehar Madni: Experimental analysis, literature review, data interpretation, writing of initial draft; Aisha Rafique, Muhammad Usama Munir and Mahpara Gondal: Literature review, data interpretation, writing initial draft; Muhammad Sajid Hamid Akash and Kanwal Rehman:

Study design, experimental validation, formal analysis, supervision, writing and reviewing of the final draft.

Funding
No funding was received for this study.

Data availability statement
The datasets generated and/or analyzed during the current study are available from the corresponding author on reasonable request.

Ethical approval
The study was approved by the Government College University, Faisalabad, Pakistan GCUF Ethical Review Committee (GCUF/ERC/542).

Conflict of interest
The authors declare no conflict of interest.

REFERENCES

Ahn S, Kearbey JD, Li CM, Duke III B, Miller D and Dalton JT (2011). Biotransformation of a novel antimitotic agent, I-387, by mouse, rat, dog, monkey and human liver microsomes and *in-vivo* pharmacokinetics in mice. *Drug Metab Dispos*., **39**(4): 636–643.

Akash MSH and Rehman K (2020). Ultraviolet-visible (UV–VIS) spectroscopy. In: *Essentials of Pharmaceutical Analysis*, *Springer Nature*. pp. 29–56.

Akash MSH, Yaqoob A, Rehman K, Imran M, Assiri MA, Al-Rashed F, Al-Mulla F, Ahmad R and Sindhu S (2023). Metabolomics: A promising tool for deciphering metabolic impairment in heavy metal toxicities. *Front. Mol. Biosci.*, **10**: 1218497.

Babalola BA, Malik M, Olowokere O, Adebesin A and Sharma L (2025). Indoles in drug design and medicinal chemistry. *Eur J Med Chem Rep.*, **13**: 100252.

Djoumbou-Feunang Y, Fiamoncini J, Gil-de-la-Fuente A, Greiner R, Manach C and Wishart DS (2019). Biotransformer: A comprehensive computational tool for small molecule metabolism prediction and metabolite identification. *J Cheminform,* **11**(1): 2.

Gondal M, Akash MSH and Rehman K (2025). Integrated *in-vivo* and *in-silico* ADMET and metabolomic profiling of basil seed bioactives methyl eugenol and linalool. *Pak J Pharm Sci.*, **38**(4): 1254-1271.

Gondal M, Akash MSH, Kamal S and Rehman K (2025). Metabolomic and biochemical evaluation of linalool and methyl eugenol as natural alternatives to varenicline in nicotine-induced metabolic dysfunction. *Naunyn Schmiedebergs Arch Pharmacol.*, **399**(3): 4043-4065.

Guengerich FP (2018). Mechanisms of cytochrome P450-catalyzed oxidations. *ACS Catal.*, **8**(12): 10964–10976.

Karnakar N, Ramana H, Amani P, Tharun DS, Nagaraju M and Sharma SB (2020). Analytical method development and validation of diclofenac sodium by UV-visible spectroscopy using AUC method. *Spectroscopy.*, **2**: 3.

Lai Y, Chu X, Di L, Gao W, Guo Y, Liu X and Ding X (2022). Recent advances in the translation of drug metabolism and pharmacokinetics science for drug discovery and development. *Acta Pharm Sin B*, **12**(6): 2751–2777.

Madni S and Akash MSH (2025). Integrated metabolomic insights and biochemical profiling of indole-3-butyric acid hydrazones in mitigating heavy metal-induced oxidative and metabolic dysregulation through Nrf2 pathway activation. *Arab J Chem.*, **18:** 5302025

Madni S, Akash MSH and Kamal S (2025). Synthesis and characterization of indole-3-butyric acid-based hydrazones: From multifunctional enzyme inhibition to therapeutic potential for drug development. *Naunyn Schmiedebergs Arch Pharmacol.*, **399**(3): 2189-2225.

Munir MU, Akash MSH and Rehman K (2025). Synthesis, characterization and biological evaluation of indole-3-acetic acid-based hydrazone derivatives. *J Mol Struct.*, **1329**: 141442.

Organisation for Economic Co-operation and Development (OECD) (2001). *OECD Guideline* **425***: Acute Oral Toxicity—Up-and-Down Procedure*. Paris: OECD.

Rafique A, Akash MSH and Rehman K (2025). Exploring the therapeutic potential of benzodioxane carboxylic acid-based hydrazones: Structural, computational and biological insights. *Arab J Chem.*, **18**: 1292025

Rafique A, Rehman K, Kamal S and Akash MSH (2025). Integrated ADME, metabolomics and multi-target docking of novel methoxy- and thiophene-substituted benzodioxane hydrazones. *Naunyn Schmiedebergs Arch Pharmacol.*, https://doi.org/10.1007/s00210-025-04886-2.

Tariq MH, Naureen H, Abbas N and Akhlaq M (2015). Development and validation of a method for the analysis of vancomycin in human serum using ultracentrifuge protein precipitation and UV spectroscopy. *Lat Am J Pharm.*, **34**(8): 1489–1496.

Wishart DS, Tian S, Allen D, Oler E, Peters H, Lui VW and Metz TO (2022). Biotransformer 3.0: A web server for accurately predicting metabolic transformation products. *Nucleic Acids Res.*, **50**(W1): W115–W123.